Geophysical Research Letters

RESEARCH LETTER
10.1029/2023GL103105

Extreme Smog Challenge of India Intensified by Increasing Lower Tropospheric Stability

Ritesh Gautam[1], Piyushkumar N. Patel[2,3], Manoj K. Singh[4], Tianjia Liu[5], Loretta J. Mickley[6], Hiren Jethva[7,8], and Ruth S. DeFries[9]

[1]Environmental Defense Fund, Washington, DC, USA, [2]NASA Jet Propulsion Laboratory, California Institute of Technology, Pasadena, CA, USA, [3]Oak Ridge Associated Universities, Oak Ridge, TN, USA, [4]School of Engineering, University of Petroleum and Energy Studies, Dehradun, India, [5]Department of Earth and Planetary Sciences, Harvard University, Cambridge, MA, USA, [6]John A. Paulson School of Engineering and Applied Sciences, Harvard University, Cambridge, MA, USA, [7]Morgan State University, Baltimore, MD, USA, [8]NASA Goddard Space Flight Center, Greenbelt, MD, USA, [9]Department of Ecology, Evolution, and Environmental Biology, Columbia University, New York, NY, USA

Abstract Extreme smog in India widely impacts air quality in late autumn and winter months. While the links between emissions, air quality and health impacts are well-recognized, the association of smog and its intensification with climatic trends in the lower troposphere, where aerosol pollution and its radiative effects manifest, are not understood well. Here we use long-term satellite data to show a significant increase in aerosol exceedances over northern India, resulting in sustained atmospheric warming and surface cooling trends over the last two decades. We find several lines of evidence suggesting these aerosol radiative effects have induced a multidecadal (1980–2019) strengthening of lower tropospheric stability and increase in relative humidity, leading to over fivefold increase in poor visibility days. Given this crucial aerosol-radiation-meteorological feedback driving the smog intensification, results from this study would help inform mitigation strategies supporting stronger region-wide measures, which are critical for solving the smog challenge in India.

Plain Language Summary Severe air pollution in India and its impacts on air quality and public health are worsening. Extreme smog episodes are frequently observed in northern India associated with the highest aerosol concentrations and hazardous visibility conditions. It is well-known that anthropogenic emissions directly affect pollution, but it remains unclear from an observational perspective how the stability of the lower troposphere, where aerosol pollution builds up, impacts the long-term evolution of smog. Using a multidecadal analysis of satellite, ground and reanalysis data sets, here we show sustained intensification of extreme smog associated with the strengthening of lower tropospheric stability, potentially amplified by aerosol-induced atmospheric warming. Solving the smog crisis in India is increasingly critical given the strongly linked aerosol-radiation-meteorological interactions.

Ritesh Gautam and Piyushkumar N. Patel contributed equally to this work.

Key Point:

- Past 40-year observations reveal aerosol-induced radiation-meteorological feedbacks have intensified extreme smog in India

Supporting Information:

Supporting Information may be found in the online version of this article.

Correspondence to:

R. Gautam,
rgautam@edf.org

Citation:

Gautam, R., Patel, P. N., Singh, M. K., Liu, T., Mickley, L. J., Jethva, H., & DeFries, R. S. (2023). Extreme smog challenge of India intensified by increasing lower tropospheric stability. *Geophysical Research Letters*, *50*, e2023GL103105. https://doi.org/10.1029/2023GL103105

Received 31 JAN 2023
Accepted 21 MAY 2023

1. Introduction

Air pollution in India severely impacts air quality, public health and economy in one of the world's most densely populated regions (Chakrabarti et al., 2019; Chowdhury et al., 2019; Pandey et al., 2021; Ravishankara et al., 2020; Venkataraman et al., 2018). Persistent agricultural fires during late autumn period (Balwinder-Singh et al., 2019; Bikkina et al., 2019; Cusworth et al., 2018; Jethva et al., 2019; Kumar et al., 2020; Liu et al., 2021; Shyamsundar et al., 2019) and widespread winter haze (Gautam et al., 2007; Ghude et al., 2017; Gunthe et al., 2021; Nair et al., 2020; Ojha et al., 2020; Pan et al., 2015; Venkataraman et al., 2019) contribute to the extreme smog over south Asia, especially affecting entire northern India. The late autumn and winter months are the worst smog periods, resulting in the largest degradation of air quality in the Indo-Gangetic Plains (IGP), where nearly one-seventh of the world's population lives across northern India, Pakistan, Nepal and Bangladesh.

In recent years, northern India has witnessed some of the most intense smog spells with extremely low visibility and hazardous air quality. The persistent smog invariably attracts heightened public and media attention (CNN, 2019) owing to the anomalous levels of fine particulate matter ($PM_{2.5}$) recorded between November and January, every year. For instance, daily $PM_{2.5}$ concentrations during agricultural burning, frequently exceed 200 $\mu g/m^3$, an order of magnitude larger than the World Health Organization's air quality guideline (Balwinder-Singh et al., 2019; CNN, 2019; Cusworth et al., 2018; Jethva et al., 2019). In addition to health and economic impacts of pollution (Chakrabarti et al., 2019; Chowdhury et al., 2019; Pandey et al., 2021; Ravishankara et al., 2020; Venkataraman

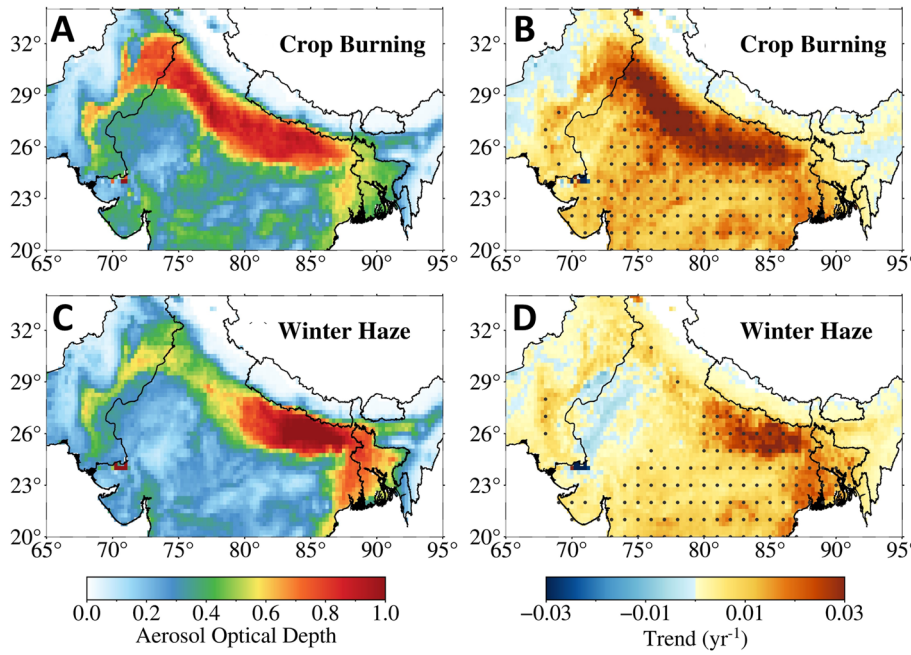

Figure 1. Aerosol distribution and trends over south Asia during the last two decades using satellite data. Aerosol optical depth (AOD) for crop burning (November) and winter haze (December–January) periods in (a) and (c), averaged from 2002 to 2019, using Aqua/MODIS observations. The AOD (unitless) is largest along the Indo-Gangetic Plains indicated by the warm shading. The corresponding linear trends in AOD (yr^{-1}) are shown in (b) and (d), with dots indicating statistical significance of trends at 95% confidence level.

et al., 2018), impacts of smog include prolonged delays/cancellations of trains and flights, and even vehicular accidents in northern India (Gautam et al., 2007; National Geographic, 2017; Pan et al., 2015).

While the worsening air quality in India has deservedly received growing attention, linkages between smog intensification and climatic trends in the lower troposphere where aerosol pollution occurs, are not understood well. On the other hand, it is well known that sunlight-absorbing aerosols lead to atmospheric warming and surface cooling via aerosol radiative effects (Ramanathan et al., 2001), thereby increasing the stability of lower troposphere by inducing a temperature inversion (An et al., 2019; Li et al., 2017). A stable lower troposphere implies reduced dispersion of pollutants leading to further accumulation of aerosols in the shallow boundary layer. Here, from an observational perspective, we examine lower-tropospheric changes during the last 40 years to investigate such aerosol-radiation-meteorological feedbacks for gaining new insights into the extreme smog problem in northern India and unraveling its long-term intensification.

2. Results

2.1. Trends in Aerosol-Induced Atmospheric Warming and Surface Cooling

We start with characterizing aerosol trends in northern India, where much of the agricultural burning occurs in the northwestern state of Punjab, the so-called breadbasket of the country and among the largest producing rice and wheat crop states nationally. Figure 1 shows the long-term climatology of satellite-derived aerosol optical depth (AOD), an indicator of aerosol loading, over south Asia averaged during the last two decades from MODIS observations (see data sets description in Supporting Information S1). The spatial distribution of AOD indicates pronounced enhancement in the IGP, along the southern edge of the Himalaya. November is the dominant crop burning month in recent years when peak fire activity and subsequent aerosol loading has increased (Jethva et al., 2019; Liu et al., 2021) and is separately shown from December–January mean (winter haze period) (Figure 1). We find accelerated upward trends in November AOD, which are higher by a factor of >3.5 relative to the annual-mean trend over northern India (Figure S1 in Supporting Information S1), leading to a ∼90% increase in November from 2002 to 2019 (Figure 2a).

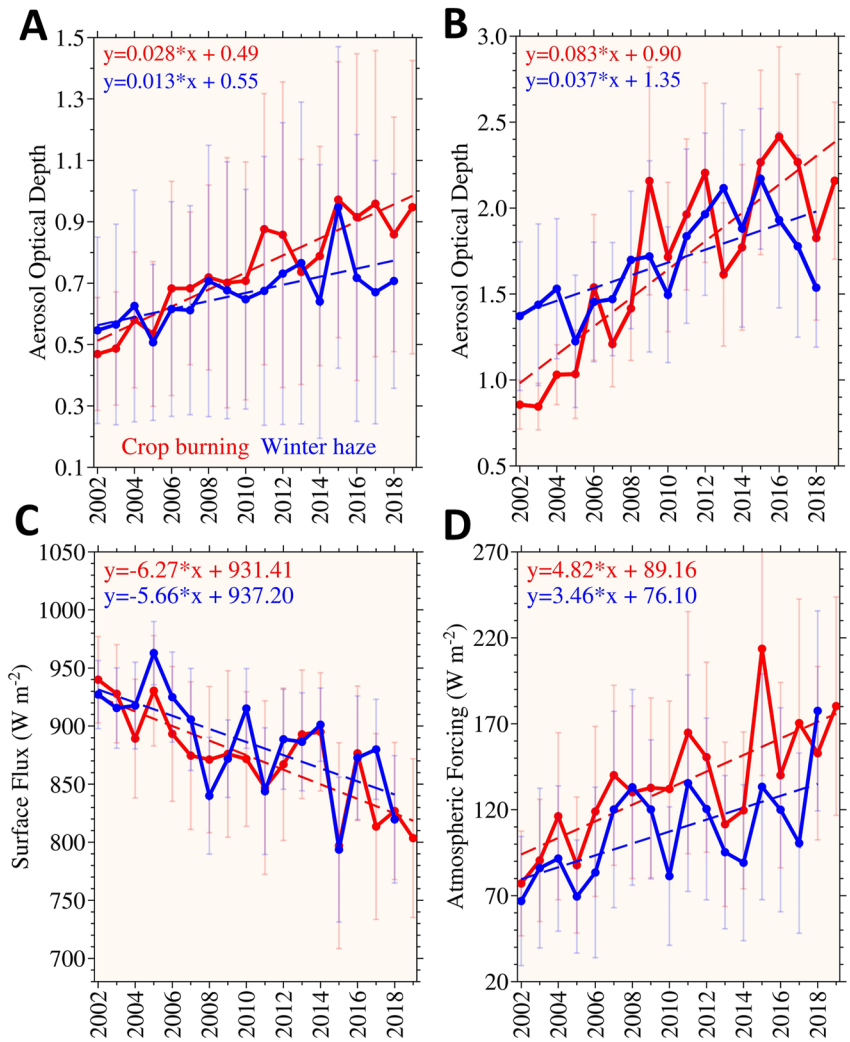

Figure 2. Trends in aerosol extremes, aerosol-induced surface cooling and atmospheric warming. Time series and linear trends for (a) mean and (b) exceedance aerosol optical depth, averaged over the Indo-Gangetic Plains for crop burning (red) and winter haze (blue) periods from 2002 to 2019. The corresponding trends in cloud-free collocated instantaneous shortwave fluxes, derived from Aqua/CERES observations, are shown in (c) surface cooling (W/m^2) and (d) atmospheric forcing (W/m^2) averaged over northern India. Error bars indicate ±1 standard deviation.

In order to characterize changes in extreme smog, we show AOD exceedances (mean of daily pixel-level data found above +1 standard deviation of the spatial mean AOD; see data sets section in Supporting Information S1) indicating an even larger increase of ~140% in November over northern India (Figure 2b). Recent studies have reported upward trends in AOD over northern India during the dry season encompassing post-monsoon and winter periods (Dey et al., 2020; Jethva et al., 2019; Liu et al., 2021; Prijith & Sai, 2022). This upsurge appears consistent with increase in agricultural fire activity, attributed to a government-mandated delay in transplanting of rice seedlings (contributing to increased burning in a shorter timespan) and expanded crop productivity in Punjab (Balwinder-Singh et al., 2019; Cusworth et al., 2018; Jethva et al., 2019; Liu et al., 2021). With respect to winter months, northern India experiences the largest aerosol loading (AOD > 0.8) over central-eastern IGP (Figure 1c), where population density is the highest across states of eastern Uttar Pradesh, Bihar and West Bengal. The winter smog is known to be associated with a shallow boundary layer, frequent temperature inversion, light winds and high relative humidity (RH) (Gautam et al., 2007; Ghude et al., 2017; Nair et al., 2020; Ojha et al., 2020; Pan et al., 2015; Venkataraman et al., 2019). Similar to November, although smaller in magnitude, we find significant positive trends in winter AOD (Figures 1d and 2a), which are >1.5 times higher than the annually-averaged trend (Figure S1 in Supporting Information S1). There is a >40% rise in winter aerosol exceedances during the last two

decades (Figure 2b), with the largest increase of ∼60% in central-eastern IGP (Figure 1d). We also find upward trends in ground-based and other satellite data sets (Figures S2–S4 in Supporting Information S1), during both crop burning and winter haze, supporting the observation of intensification in aerosol pollution as detected in multiple disparate measurements.

How does the increased aerosol pollution impact the regional radiation budget? We analyze the direct radiative effect of aerosols (Satheesh & Ramanathan, 2000), specifically to characterize the impact of increasing AOD, observed in the last two decades, on surface cooling and atmospheric warming trends using solar radiation fluxes from CERES satellite observations (see methods and data sets in Supporting Information S1). A consistent increase is found in top-of-atmosphere (TOA) flux (Figure S5 in Supporting Information S1) and a reduction in surface-reaching radiation (implying surface cooling), corresponding to cloud-free aerosol-laden observations during the last two decades (Figure 2c). An example of the relationship between collocated AOD and radiation fluxes (Figure S6 in Supporting Information S1), indicates a positive aerosol-induced effect at the TOA (brightening) and negative effect at surface (cooling). The surface cooling associated with crop burning and winter haze is evident across the IGP, leading to over 15%–25% instantaneous reduction in solar insolation (Figures S6 and S7 in Supporting Information S1).

Our central finding in the radiative effects analysis is the net increase in aerosol-induced surface cooling over the last two decades (over 10% increase in surface cooling from 2002 to 2019 as shown in Figure 2c), is twice as large compared to the corresponding increase in TOA flux (∼5% increase in TOA flux from 2002 to 2019 as shown in Figure S5 in Supporting Information S1). This disparity implies that considerably less radiation is being reflected at TOA over the past two decades as a result of significant solar absorption within the aerosol layer, in turn causing the large surface cooling anomaly. This result is significant because here we report aerosol-induced "trends" in TOA fluxes and surface cooling over the last two decades, which builds on previous aerosol-radiation studies that have reported large "absolute" differences in TOA and surface fluxes over 1–2 years (Satheesh & Ramanathan, 2000). Our study therefore highlights, from a long-term trend perspective, the radiative effects of continued degradation of air quality in northern India during late autumn crop burning and winter haze periods. This is consistent with the low aerosol single scattering albedo in northern India (Kaskaoutis et al., 2014; Li et al., 2015), indicative of an absorbing aerosol layer. The resulting aerosol-induced absorption (Figure 2d) and atmospheric heating rate (Figure S9 in Supporting Information S1) is largely confined to the lowest ∼1.5 km of the troposphere, where most of the aerosol layer resides during late autumn-winter in northern India, as indicated by spaceborne lidar observations (Figure S10 in Supporting Information S1). Overall, concurrent with enhanced surface cooling, there is a 70%–80% increase in aerosol-induced lower tropospheric warming over the last two decades (Figures 2c and 2d), suggesting an increasing tendency toward a stable lower troposphere, which favors buildup of aerosol pollution in the shallow boundary layer where emissions from agricultural fires and other anthropogenic sources occur.

In addition, we analyzed AOD and radiative forcing data during pre-monsoon (March–May) and monsoon (June–September) seasons in order to investigate whether similar trends exist relative to the crop burning and winter haze periods. Figure S1 (and Table S1) in Supporting Information S1 show neutral trends in pre-monsoon and monsoon seasons, from 2002 to 2019, that are statistically not significant for AOD (both mean and exceedance AOD). Subsequently, Figure S8 (and Table S1) in Supporting Information S1 shows a clear lack of trends for aerosol-induced surface cooling and atmospheric forcing, that are statistically not significant, during both pre-monsoon and monsoon seasons. These results are in sharp contrast with respect to the observed increasing AOD, surface cooling and atmospheric forcing trends consistently found for November and December–January. Overall, the observed annual mean increasing trend in AOD is mainly contributed by the AOD increase during crop burning and winter haze periods, despite the neutral or lack of trends found in pre-monsoon and monsoon seasons. These results strengthen our argument about smog intensification during November–January, consistent with the prevailing meteorology where lower tropospheric conditions during late autumn and winter period are favorable for the accumulation and persistence of aerosol pollution in the shallow boundary layer.

2.2. Strengthening of Lower Tropospheric Stability and Intensification of Smog

With aerosol-induced radiative effects evident in the observed lower tropospheric warming and surface cooling, we then investigate whether long-term changes in atmospheric stability and related meteorological parameters have occurred, in turn amplifying the smog intensification. Figure 3 shows the climatology and trends of lower

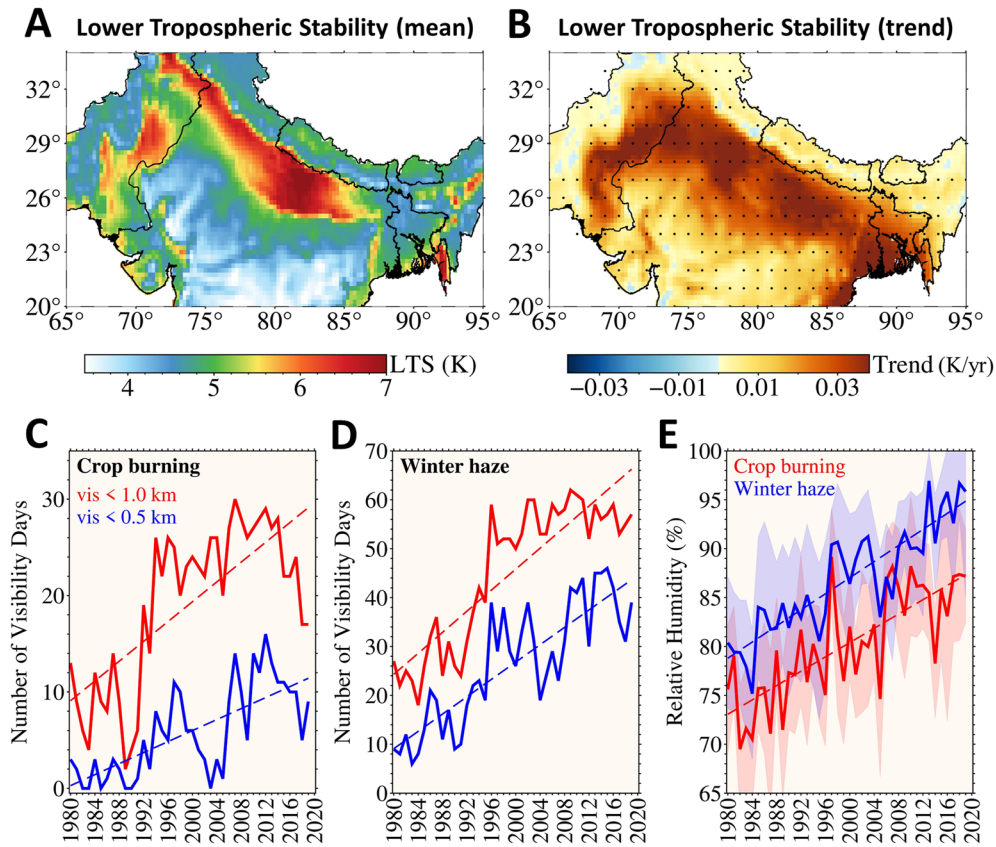

Figure 3. Lower tropospheric stability (LTS) and long-term trends in smog. The LTS is shown as (a) the multidecadal average and (b) spatial trend, from November–January for the period 1980–2019, with significantly increasing LTS along the Indo-Gangetic Plains. Dots in (b) indicate statistical significance of trends at 95% confidence level. Number of visibility days during (c) crop burning in November (out of 30 days) and (d) winter haze in December–January (out of 62 days) over Delhi. Visibility <1 km is shown in red and <0.5 km in blue. The monthly mean relative humidity (e) is shown for crop burning (red) and winter haze (blue) periods. Shading represents ±1 standard deviation.

tropospheric stability (LTS) (Wood & Bretherton, 2006), a measure of the strength of temperature inversion that caps the planetary boundary layer (PBL) (see data sets section in Supporting Information S1). The IGP emerges under a strong LTS influence during late autumn and winter, based on the past four decades of meteorological data (Figure 3a; Figure S11 in Supporting Information S1). The enhanced LTS is particularly evident over northern India, as part of an overall stable lower-tropospheric feature. We find a significant and sustained upward trend leading to an 18%–25% increase in LTS over northern India from 1980 to 2019 (Figure 3b; Table S2 in Supporting Information S1).

Coincidentally, the number of poor visibility days (defined here as visibility <1000 m) has increased fivefold over northern India during November and >2 times during December–January over the last 40 years (Figure S12 in Supporting Information S1). This worsening trend is even severe for days with much lower visibility (<500 m), indicating a factor of >9 increase during the crop burning period and a fivefold increase in winter. Over Delhi, where pollution levels are among the highest in the world, the smog has undergone significant intensification (at least a fivefold increase for visibility <500 m), with poor visibility largely dominating the late autumn-winter periods since the 1990s (Figures 3c and 3d; Table S2 in Supporting Information S1). The degrading visibility is accompanied by a systematic 20% increase in near-surface RH, over the last four decades, with high RH (85%–95%) observed in recent years (Figure 3e).

Overall, there appears to be an aerosol-radiation-meteorological feedback mechanism playing a potentially crucial role toward smog intensification whereby aerosol-induced atmospheric warming may strengthen the stability of the lower troposphere. This association is elucidated in Figure 4 where aerosol-induced atmospheric warming is shown as a function of AOD derived from co-located CERES and MODIS satellite observations,

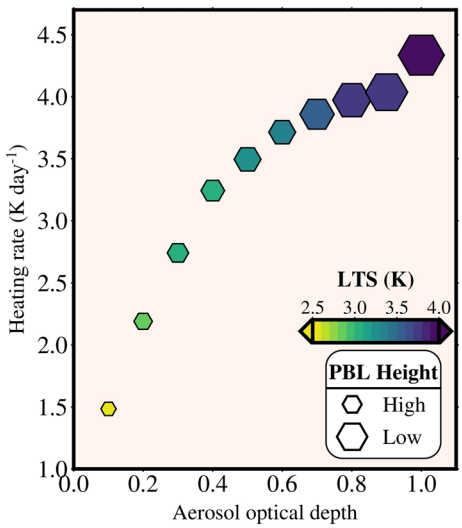

Figure 4. Aerosol-Radiation-Meteorological interactions over northern India. Aerosol-induced atmospheric heating rate (K/day^{-1}) is shown as a function of aerosol optical depth (AOD) derived from CERES and MODIS satellite observations, corresponding to lower tropospheric stability (LTS) (indicated by shading of the hexagon symbols) and planetary boundary layer (PBL) height (meters) indicated by the size of the colored symbols. The aerosol-induced heating rate increases with aerosol optical depth along with an increase in LTS which strengthens at lower PBL heights (shallow boundary layer) and weakens at larger PBL heights (deeper boundary layer). The aerosol-radiation-meteorological analysis presented here is for the November–January period (i.e., covering the crop burning and winter haze months) from 2002 to 2019.

respectively; whereas the corresponding changes in LTS also co-located with aerosol-induced warming are indicated by the shading of the hexagon symbols. Based on daily observations aggregated from 19 years (2002–2019), we find that as the aerosol loading increases by a factor of 10 (from AOD = 0.1 to AOD = 1.0), averaged over the IGP during the crop burning and winter haze periods, the aerosol-induced warming increases by ∼170%, whereas the corresponding LTS also systematically increases by ∼50%. At the same time, the co-located PBL over the IGP becomes systematically shallower by ∼30% (indicated by the size of the colored symbols), overlapping with simultaneous increases in AOD, aerosol-induced atmospheric warming and stability of lower troposphere (Figure 4).

Altogether, as the aerosol-induced warming increases (between the top of the shallow boundary layer and ∼1,000 m above m.s.l., more information is included in Supporting Information S1 methods section (i) aerosol radiative forcing), the stability of lower troposphere is found to significantly strengthen along with the contraction of PBL (as indicated by lower PBL heights at high AOD and vice versa). Increased stability means capping of pollutants and further increase in aerosol loading in the shallow PBL; at the same time entrainment of dry air from the free troposphere decreases, causing enhanced moisture availability in the PBL and higher RH (Li et al., 2017; Nair et al., 2020). The increase in RH enhances aerosol scattering mediated by the hygroscopic growth of aerosols, and promotes formation of secondary aerosols, further exacerbating the severity of smog (An et al., 2019; Pan et al., 2015). Coincidentally, we found a strong association between RH and poor visibility that indicates a higher correlation (r: 0.77–0.85, p-value << 0.01) for days with visibility <500 m in both November and December–January months (Figure 5a), relative to visibility <1000 m, supporting the observation of enhanced visibility degradation under humid conditions. We also find indication of the contraction of PBL in recent decades (see Figures S13 and S16 and methods in Supporting Information S1), suggesting a moistened shallow boundary layer favorable for persistence of smoggy conditions. These distinct concomitant associations may not necessarily be construed as a cause-and-effect relationship, but they reveal observational insights related to aerosol-radiation-meteorological feedbacks (refer to process-level schematic shown in Figure S14 in Supporting Information S1), based on a synthesis of disparate variables and data sets, which strengthen the long-term intensification of smog.

The increase in RH may also in part be linked to the increase in irrigated area in the IGP; irrigation in India has expanded 2–3 times since the 1970s and may contribute to the enhanced moisture in the PBL (Ambika & Mishra, 2020). The increase in irrigation over northern India may have contributed to an increase in soil moisture and decrease in land surface temperature, as seen in reanalysis data and satellite observations in the last four decades, respectively (Ambika & Mishra, 2020). Such changes in the shallow boundary layer can favor the hygroscopic growth of aerosols supporting the development of smog, as discussed earlier. Regardless of the cause, smog intensification appears to be amplified by aerosol-radiation-meteorological feedbacks, as observed in the increasing trends of aerosol-induced atmospheric warming and surface cooling, along with the long-term strengthening of LTS and concurrent trends in RH and visibility degradation during the last 40 years.

3. Discussion

It is noteworthy that extreme smog episodes in November, coinciding with agricultural burning, arrive in advance of the peak winter smog season in the IGP. As an illustration of the aerosol-radiation-meteorological coupling, Figure 5c shows the evolution of a dense smog spell in satellite imagery with thick haze around the beginning of November 2017, transforming into foggy conditions that altogether persisted for almost three weeks. The smog was so severe across northern India that the peak $PM_{2.5}$ concentrations reached ∼1,000 μg/m^3 in Delhi, prompting the closure of 4,000 schools (Shyamsundar et al., 2019) and a major international airliner to suspend its flight operations into the city (CNN, 2017). In another recent smog-filled episode, an international cricket match (most

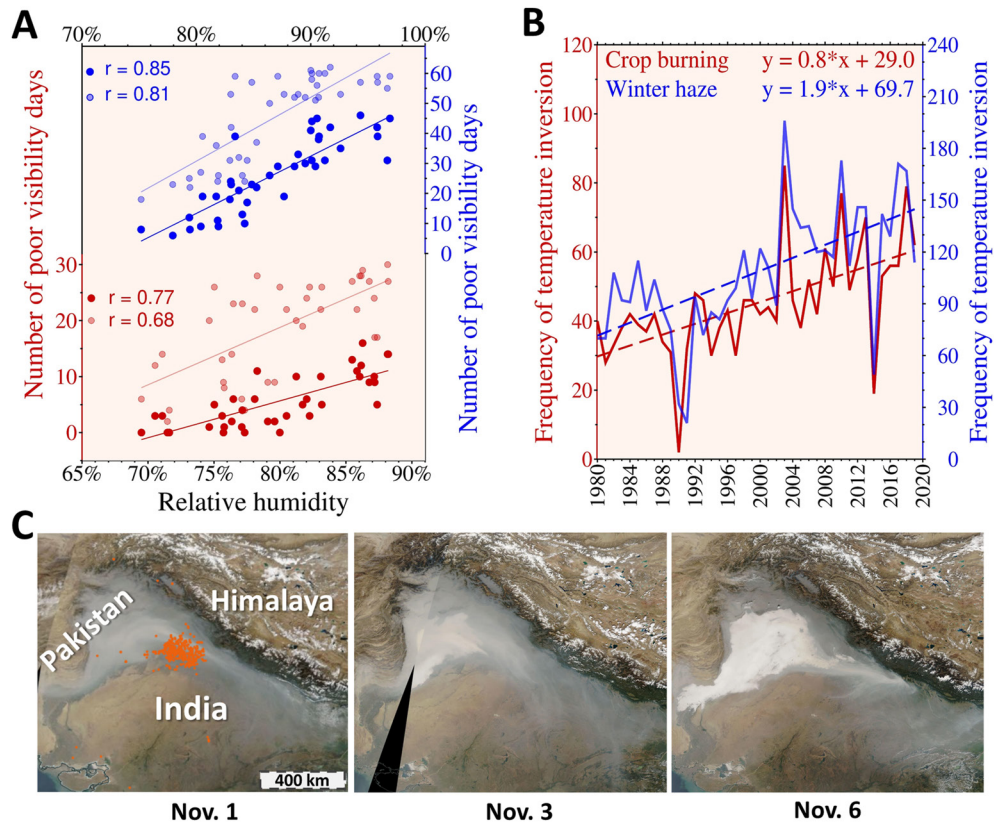

Figure 5. Long-term evolution of smog blanketing southern Asia. (a) Correlation between number of poor visibility days and monthly mean relative humidity for the period 1980–2019, based on surface meteorological observations over Delhi, for November (red color, left *y*-axis) and December–January (blue color, right *y*-axis). The number of visibility days <1 km is shown in light red (November) and light blue (December–January), whereas number of visibility days <0.5 km are shown in dark red (November) and dark blue (December–January). Correlation is higher for visibility <0.5 km for both time periods (*r*: 0.77–0.85, *p*-value << 0.01) suggesting enhanced poor visibility degradation under humid conditions. (b) Time series and linear trends in the frequency of temperature inversion (i.e., monthly count of the total number of detected inversion layers, in daily radiosonde observations) in the lower troposphere over Delhi from 1980 to 2019, for November (red) and December–January (blue). (c) An illustrative depiction of the evolution of smog in the Indo-Gangetic Plains, south of the Himalaya, encompassing Pakistan, northern India and Nepal. Satellite imagery (Terra/MODIS) is from 1, 3, 6 November 2017 acquired at ~10:30 a.m. local-time. Orange dots on 1 November show fire detections from Aqua/MODIS satellite observations (1:30 p.m. local-time).

popular sport in south Asia) was halted probably for the first time in the sports' history due to smog, with players visibly sick and wearing pollution masks on the field (Guardian, 2017). This intense degradation in air quality and visibility could have been amplified by a pronounced temperature inversion and high RH in the lower troposphere (Figure S14 in Supporting Information S1). We also analyzed 40 years of radiosonde observations of daily temperature profiles and found a twofold increase in the frequency of lower tropospheric temperature inversion (Figure 5b; Figure S15 and Table S2 in Supporting Information S1), consistent with upward trends in LTS, visibility degradation and RH (Figure 3).

Such extreme events serve as examples of the heightened attention the smog problem has increasingly received. On the other hand, there seems to be a lack of clarity regarding sources and transport mechanisms across states and countries in south Asia (Hindu, 2020; Miro et al., 2019), which could be limiting effective measures to address the smog. In addition, the possible role of climate variability in contributing to poor ventilation conditions, suggested as conducive for extreme haze formation in China (Zou et al., 2017), may be worth investigating for studying severe smog episodes in India.

The government of India, in October 2020, promulgated a major commission on air quality management in the national capital region (NCR) around Delhi and adjoining areas (The Gazette of India, 2020). This initiative

distinctly recognizes the air pollution challenge in NCR; where adjoining areas are defined as "where any source of pollution is located causing adverse impact of air quality in the NCR" (The Gazette of India, 2020). As our results indicate, the increasing aerosol pollution and radiative impacts, clearly extend beyond NCR (<60 million population) and encompass the whole of northern India, affecting both the urban and the vast rural populations (>600 million population of Indian states in the IGP).

While reductions in emissions are known to have led to significant air quality improvements across broad regions of Europe, North America, and East Asia (Hammer et al., 2020; Vautard et al., 2009), the long-term rise in extreme smog over northern India is particularly concerning and in turn provides an opportunity to strengthen mitigation action. The northern Indian region, as part of the broader IGP, lies in a valley-type terrain immediately south of the towering Himalaya and so is naturally vulnerable to pollution build-up. Given the likely role of aerosol-radiation-meteorological feedbacks in worsening the widespread smog, expanding upon current air quality improvement efforts by accounting for pollution sources and transport processes across entire northern India, will support the development of a region-wide mitigation strategy.

Conflict of Interest

The authors declare no conflicts of interest relevant to this study.

Data Availability Statement

All data underlying this study are available in the public domain. The MODIS data used in this study are available via http://dx.doi.org/10.5067/MODIS/MYD04_L2.006 and CERES data are available via https://doi.org/10.5067/Aqua/CERES/SSF-FM3_L2.004A. We have provided links to the various data access portals in the Supporting Information S1 Appendix Data sets description section for each of the satellite data set, ground-based observations and modeling-based reanalysis data sets used in this study.

Acknowledgments
We thank the various science and data processing teams for providing access to the satellite, ground-based and reanalysis datasets used in this study.

References

Ambika, A. K., & Mishra, V. (2020). Substantial decline in atmospheric aridity due to irrigation in India. *Environmental Research Letters*, *15*(12), 124060. https://doi.org/10.1088/1748-9326/abc8bc

An, Z., Huang, R. J., Zhang, R., Tie, X., Li, G., Cao, J., et al. (2019). Severe haze in northern China: A synergy of anthropogenic emissions and atmospheric processes. *Proceedings of the National Academy of Sciences of the United States of America*, *116*(18), 8657–8666. https://doi.org/10.1073/pnas.1900125116

Balwinder-Singh, McDonald, A. J., Srivastava, A. K., & Gerard, B. (2019). Tradeoffs between groundwater conservation and air pollution from agricultural fires in northwest India. *Nature Sustainability*, *2*(7), 580–583. https://doi.org/10.1038/s41893-019-0304-4

Bikkina, S., Andersson, A., Kirillova, E. N., Holmstrand, H., Tiwari, S., Srivastava, A. K., et al. (2019). Air quality in megacity Delhi affected by countryside biomass burning. *Nature Sustainability*, *2*(3), 200–205. https://doi.org/10.1038/s41893-019-0219-0

Chakrabarti, S., Khan, M. T., Kishore, A., Roy, D., & Scott, S. P. (2019). Risk of acute respiratory infection from crop burning in India: Estimating disease burden and economic welfare from satellite and national health survey data for 250 000 persons. *International Journal of Epidemiology*, *48*(4), 1113–1124. https://doi.org/10.1093/ije/dyz022

Chowdhury, S., Dey, S., Guttikunda, S., Pillarisetti, A., Smith, K. R., & di Girolamo, L. (2019). Indian annual ambient air quality standard is achievable by completely mitigating emissions from household sources. *Proceedings of the National Academy of Sciences of the United States of America*, *166*(22), 10711–10716. https://doi.org/10.1073/PNAS.1900888116/SUPPL_FILE/PNAS.1900888116.SAPP.PDF

CNN. (2017). United suspends flights to smog-filled Delhi. Retrieved from https://money.cnn.com/2017/11/10/news/delhi-pollution-united-flights/index.html

CNN. (2019). New Delhi is choking on smog and there's no end in sight. Retrieved from https://www.cnn.com/2019/11/04/india/delhi-india-smog-pollution-intl-hnk/index.html

Cusworth, D. H., Mickley, L. J., Sulprizio, M. P., Liu, T., Marlier, M. E., Defries, R. S., et al. (2018). Quantifying the influence of agricultural fires in northwest India on urban air pollution in Delhi, India. *Environmental Research Letters*, *13*(4), 044018. https://doi.org/10.1088/1748-9326/aab303

Dey, S., Purohit, B., Balyan, P., Dixit, K., Bali, K., Kumar, A., et al. (2020). A satellite-based high-resolution (1-km) ambient $PM_{2.5}$ database for India over two decades (2000–2019): Applications for air quality management. *Remote Sensing*, *12*(23), 3872. https://doi.org/10.3390/RS12233872

Gautam, R., Hsu, N. C., Kafatos, M., & Tsay, S. C. (2007). Influences of winter haze on fog/low cloud over the Indo-Gangetic plains. *Journal of Geophysical Research*, *112*(5), 5207. https://doi.org/10.1029/2005JD007036

Ghude, S. D., Bhat, G. S., Prabhakaran, T., Jenamani, R. K., Chate, D. M., Safai, P. D., et al. (2017). Winter fog experiment over the Indo-Gangetic plains of India. *Current Science*, *112*(4), 767–784. https://doi.org/10.18520/cs/v112/i04/767-784

Guardian, T. (2017). Pollution stops play at Delhi Test match as bowlers struggle to breathe. Retrieved from https://www.theguardian.com/world/2017/dec/03/pollution-stops-play-at-delhi-test-match-as-bowlers-struggle-to-breathe

Gunthe, S., Liu, P., Panda, U., Raj, S. S., Sharma, A., Darbyshire, E., et al. (2021). Enhanced aerosol particle growth sustained by high continental chlorine emission in India. *Nature Geoscience*, *14*(2), 77–84. https://doi.org/10.1038/s41561-020-00677-x

Hammer, M. S., van Donkelaar, A., Li, C., Lyapustin, A., Sayer, A. M., Hsu, N. C., et al. (2020). Global estimates and long-term trends of fine particulate matter concentrations (1998–2018). *Environmental Science and Technology*, *54*(13), 7879–7890. https://doi.org/10.1021/acs.est.0c01764

Hindu, T. (2020). States should stop blaming each other on stubble burning, need to take it seriously: Arvind Kejriwal—The Hindu. Retrieved from https://www.thehindu.com/news/cities/Delhi/states-should-stop-blaming-each-other-on-stubble-burning-need-to-take-it-seriously-arvind-kejriwal/article32843377.ece

Jethva, H., Torres, O., Field, R. D., Lyapustin, A., Gautam, R., & Kayetha, V. (2019). Connecting crop productivity, residue fires, and air quality over northern India. *Scientific Reports*, *9*(1), 1–11. https://doi.org/10.1038/s41598-019-52799-x

Kaskaoutis, D. G., Kumar, S., Sharma, D., Singh, R. P., Kharol, S. K., Sharma, M., et al. (2014). Effects of crop residue burning on aerosol properties, plume characteristics, and long-range transport over northern India. *Journal of Geophysical Research*, *119*(9), 5424–5444. https://doi.org/10.1002/2013JD021357

Kumar, R., Ghude, S. D., Biswas, M., Jena, C., Alessandrini, S., Debnath, S., et al. (2020). Enhancing accuracy of air quality and temperature forecasts during paddy crop residue burning season in Delhi via chemical data assimilation. *Journal of Geophysical Research: Atmospheres*, *125*(17), e2020JD033019. https://doi.org/10.1029/2020JD033019

Li, Z. Z., Guo, J., Ding, A., Liao, H., Liu, J., Sun, Y., et al. (2017). Aerosol and boundary-layer interactions and impact on air quality. *National Science Review*, *4*(6), 810–833. https://doi.org/10.1093/nsr/nwx117

Li, Z. Z., Li, L., Zhang, F., Li, D., Xie, Y., & Xu, H. (2015). Comparison of aerosol properties over Beijing and Kanpur: Optical, physical properties and aerosol component composition retrieved from 12 years ground-based Sun-sky radiometer remote sensing data. *Journal of Geophysical Research*, *120*(4), 1520–1535. https://doi.org/10.1002/2014JD022593

Liu, T., Mickley, L. J., Gautam, R., Singh, M. K., DeFries, R. S., & Marlier, M. E. (2021). Detection of delay in post-monsoon agricultural burning across Punjab, India: Potential drivers and consequences for air quality. *Environmental Research Letters*, *16*(1), 014014. https://doi.org/10.1088/1748-9326/abcc28

Miro, M., Marlier, M., & Girven, R. (2019). *Transboundary environmental stressors on India-Pakistan relations: An analysis of shared air and water resources*. RAND Corporation. https://doi.org/10.7249/rr2715

Nair, V. S., Giorgi, F., & Keshav Hasyagar, U. (2020). Amplification of South Asian haze by water vapour-aerosol interactions. *Atmospheric Chemistry and Physics*, *20*(22), 14457–14471. https://doi.org/10.5194/acp-20-14457-2020

National Geographic. (2017). Pollution is so bad in India, it's causing car crashes | National Geographic—YouTube. Retrieved from https://www.youtube.com/watch?v=r_vQDa42tuM

Ojha, N., Sharma, A., Kumar, M., Girach, I., Ansari, T. U., Sharma, S. K., et al. (2020). On the widespread enhancement in fine particulate matter across the Indo-Gangetic Plain towards winter. *Scientific Reports*, *10*(1), 1–9. https://doi.org/10.1038/s41598-020-62710-8

Pan, X., Chin, M., Gautam, R., Bian, H., Kim, D., Colarco, P. R., et al. (2015). A multi-model evaluation of aerosols over South Asia: Common problems and possible causes. *Atmospheric Chemistry and Physics*, *15*(10), 5903–5928. https://doi.org/10.5194/acp-15-5903-2015

Pandey, A., Brauer, M., Cropper, M. L., Balakrishnan, K., Mathur, P., Dey, S., et al. (2021). Health and economic impact of air pollution in the states of India: The Global Burden of Disease Study 2019. *The Lancet Planetary Health*, *5*(1), e25–e38. https://doi.org/10.1016/S2542-5196(20)30298-9

Prijith, S. S., & Sai, M. V. R. S. (2022). Enhancement in free-tropospheric aerosol loading over India. *Atmospheric Environment*, *276*, 119035. https://doi.org/10.1016/J.ATMOSENV.2022.119035

Ramanathan, V., Crutzen, P. J., Kiehl, J. T., & Rosenfeld, D. (2001). Aerosols, climate, and the hydrological cycle. *Science*, *294*(5549), 2119–2124. https://doi.org/10.1126/science.1064034

Ravishankara, A. R., David, L. M., Pierce, J. R., & Venkataraman, C. (2020). Outdoor air pollution in India is not only an urban problem. *Proceedings of the National Academy of Sciences of the United States of America*, *117*(46), 28640–28644. https://doi.org/10.1073/pnas.2007236117

Satheesh, S., & Ramanathan, V. (2000). Large differences in tropical aerosol forcing at the top of the atmosphere and Earth's surface. *Nature*, *405*(6782), 60–63. https://doi.org/10.1038/35011039

Shyamsundar, P., Springer, N. P., Tallis, H., Polasky, S., Jat, M. L., Sidhu, H. S., et al. (2019). Fields on fire: Alternatives to crop residue burning in India. *Science*, *365*(6453), 536–538. https://doi.org/10.1126/science.aaw4085

The Gazette of India, E. (2020). The commission for air quality management in national capital region and adjoining areas ordinance, 1942 §. Retrieved from http://www.egazette.nic.in/WriteReadData/2020/222804.pdf

Vautard, R., Yiou, P., & van Oldenborgh, G. J. (2009). Decline of fog, mist and haze in Europe over the past 30 years. *Nature Geoscience*, *2*(2), 115–119. https://doi.org/10.1038/ngeo414

Venkataraman, C., Brauer, M., Tibrewal, K., Sadavarte, P., Ma, Q., Cohen, A., et al. (2018). Source influence on emission pathways and ambient $PM_{2.5}$ pollution over India (2015–2050). *Atmospheric Chemistry and Physics*, *18*(11), 8017–8039. https://doi.org/10.5194/ACP-18-8017-2018

Venkataraman, C., Sharma, A., Tibrewal, K., Maity, S., & Muduchuru, K. (2019). *Carbonaceous aerosol emissions sources dominate India's wintertime air quality*. EM. Retrieved from https://pubs.awma.org/flip/EM-Dec-2019/venkataraman.pdf

Wood, R., & Bretherton, C. S. (2006). On the relationship between stratiform low cloud cover and lower-tropospheric stability. *Journal of Climate*, *19*(24), 6425–6432. https://doi.org/10.1175/JCLI3988.1

Zou, Y., Wang, Y., Zhang, Y., & Koo, J.-H. (2017). Arctic sea ice, Eurasia snow, and extreme winter haze in China. *Science Advances*, *3*(3), e1602751. https://doi.org/10.1126/sciadv.1602751

References From the Supporting Information

Ding, F., Iredell, L., Theobald, M., Wei, J., & Meyer, D. (2021). PBL height from AIRS, GPS RO, and MERRA-2 products in NASA GES DISC and their 10-year seasonal mean intercomparison. *Earth and Space Science*, *8*(9), e2021EA001859. https://doi.org/10.1029/2021EA001859

Durre, I., & Yin, X. (2008). Enhanced radiosonde data for studies of vertical structure. *Bulletin of the American Meteorological Society*, *89*(9), 1257–1261. https://doi.org/10.1175/2008BAMS2603.1

Durre, I., Vose, R. S., & Wuertz, D. B. (2006). Overview of the integrated global radiosonde archive. *Journal of Climate*, *19*(1), 53–68. https://doi.org/10.1175/JCLI3594.1

Fu, Q., & Liou, K. N. (1993). Parameterization of the radiative properties of cirrus clouds. *Journal of the Atmospheric Sciences*, *50*(13), 2008–2025. https://doi.org/10.1175/1520-0469(1993)050<2008:POTRPO>2.0.CO;2

Gautam, R., Hsu, N. C., Eck, T. F., Holben, B. N., Janjai, S., Jantarach, T., et al. (2013). Characterization of aerosols over the Indochina peninsula from satellite-surface observations during biomass burning pre-monsoon season. *Atmospheric Environment*, *78*, 51–59. https://doi.org/10.1016/j.atmosenv.2012.05.038

Gilson, G. F., Jiskoot, H., Cassano, J. J., & Nielsen, T. R. (2018). Radiosonde-derived temperature inversions and their association with fog over 37 Melt seasons in east Greenland. *Journal of Geophysical Research: Atmospheres*, *123*(17), 9571–9588. https://doi.org/10.1029/2018JD028886

Hersbach, H., Bell, B., Berrisford, P., Hirahara, S., Horányi, A., Muñoz-Sabater, J., et al. (2020). The ERA5 global reanalysis. *Quarterly Journal of the Royal Meteorological Society*, *146*(730), 1999–2049. https://doi.org/10.1002/qj.3803

Hsu, N. C., Herman, J. R., & Weaver, C. (2000). Determination of radiative forcing of Saharan dust using combined TOMS and ERBE data. *Journal of Geophysical Research*, *105*(16), 20649–20661. https://doi.org/10.1029/2000jd900150

Kahl, J. D., Serreze, M. C., & Schnell, R. C. (1992). Tropospheric low-level temperature inversions in the Canadian arctic. *Atmosphere-Ocean*, *30*(4), 511–529. https://doi.org/10.1080/07055900.1992.9649453

Kato, S., Loeb, N. G., Rose, F. G., Doelling, D. R., Rutan, D. A., Caldwell, T. E., et al. (2013). Surface irradiances consistent with CERES-derived top-of-atmosphere shortwave and longwave irradiances. *Journal of Climate*, *26*(9), 2719–2740. https://doi.org/10.1175/JCLI-D-12-00436.1

Kato, S., Rose, F. G., Rutan, D. A., Thorsen, T. J., Loeb, N. G., Doelling, D. R., et al. (2018). Surface irradiances of edition 4.0 clouds and the Earth's radiant energy system (CERES) energy balanced and filled (EBAF) data product. *Journal of Climate*, *31*(11), 4501–4527. https://doi.org/10.1175/JCLI-D-17-0523.1

Kratz, D. P., Gupta, S. K., Wilber, A. C., & Sothcott, V. E. (2020). Validation of the CERES edition-4A surface-only flux algorithms. *Journal of Applied Meteorology and Climatology*, *59*(2), 281–295. https://doi.org/10.1175/JAMC-D-19-0068.1

Loeb, N. G., Manalo-Smith, N., Su, W., Shankar, M., & Thomas, S. (2016). CERES top-of-atmosphere Earth radiation budget climate data record: Accounting for in-orbit changes in instrument calibration. *Remote Sensing*, *8*(3), 182. https://doi.org/10.3390/rs8030182

McGrath-Spangler, E. L., & Molod, A. (2014). Comparison of GEOS-5 AGCM planetary boundary layer depths computed with various definitions. *Atmospheric Chemistry and Physics*, *14*(13), 6717–6727. https://doi.org/10.5194/ACP-14-6717-2014

Ricchiazzi, P., Yang, S., Gautier, C., & Sowle, D. (1998). SBDART: A research and teaching software tool for plane-parallel radiative transfer in the Earth's atmosphere. *Bulletin of the American Meteorological Society*, *79*(10), 2101–2114. https://doi.org/10.1175/1520-0477(1998)079<2101:sarats>2.0.co;2

Sayer, A. M., Hsu, N. C., Bettenhausen, C., Jeong, M. J., & Meister, G. (2015). Effect of MODIS terra radiometric calibration improvements on Collection 6 Deep blue aerosol products: Validation and terra/aqua consistency. *Journal of Geophysical Research*, *120*(23), 12157–12174. https://doi.org/10.1002/2015JD023878

Seibert, P., Beyrich, F., Gryning, S. E., Joffre, S., Rasmussen, A., & Tercier, P. (2000). Review and intercomparison of operational methods for the determination of the mixing height. *Atmospheric Environment*, *34*(7), 1001–1027. https://doi.org/10.1016/S1352-2310(99)00349-0

Seidel, D. J., Zhang, Y., Beljaars, A., Golaz, J. C., Jacobson, A. R., & Medeiros, B. (2012). Climatology of the planetary boundary layer over the continental United States and Europe. *Journal of Geophysical Research*, *117*(17), 17106. https://doi.org/10.1029/2012JD018143

Su, W., Corbett, J., Eitzen, Z., & Liang, L. (2015). Next-generation angular distribution models for top-of-atmosphere radiative flux calculation from CERES instruments: Validation. *Atmospheric Measurement Techniques*, *8*(8), 3297–3313. https://doi.org/10.5194/amt-8-3297-2015